Differential cross sections for electron impact ionization of helium

V. L. Jacobs*
Theoretical Studies Group, Goddard Space Flight Center, National Aeronautics and Space Administration, Greenbelt, Maryland 20771
(Received 8 May 1974)

Differential cross sections for electron impact ionization of helium are calculated in the Born approximation for ejected-electron energies below the $n=2$ threshold of the residual He^+ ion. The resonant features associated with the lowest-lying ^1S, ^1P, and ^1D helium autoionizing states are analyzed using the Fano line-shape formula. The angular correlation between the two outgoing electrons is expressed as a Legendre-polynomial expansion, and the coefficients are evaluated for representative energy losses and momentum transfers. For an incident-electron energy of 256.5 eV, the predicted angular distribution is in satisfactory agreement with the coincidence measurements of Ehrhardt *et al.* except near the recoil maximum.

I. INTRODUCTION

A knowledge of electron impact excitation and ionization cross sections for atomic systems is important in the interpretation of emission spectra from laboratory and astrophysical plasmas. For electron impact ionization, the Born approximation and its variants have been widely used but their validity has not been firmly established.

In 1930 Bethe[1] developed a quantum-mechanical theory, based on the Born approximation, for inelastic collisions between fast charged particles and atoms. An important concept introduced in this theory is that of the generalized oscillator strength which describes the sudden transfer of energy and momentum to the atomic system during the collision.

Inokuti[2] has given particular emphasis to the central role played by the generalized oscillator strength in providing a unified picture of high-energy atomic collision processes. Motivated by the need for a reliable test of the validity of the Born approximation, Kim and Inokuti[3-5] have employed Hylleraas bound-state wave functions in an accurate evaluation of the Bethe generalized oscillator strength for collisional transitions between low-lying discrete states of helium. The present investigation may be considered as an extension of their work to ionization continua of the helium atom.

It is well known that the Bethe generalized oscillator strength reduces to the optical-transition oscillator strength in the limit of zero momentum transfer. Burke and McVicar[6] have evaluated the differential oscillator strength for photoionization of helium below the $n=2$ threshold of He^+, using a Hylleraas ground-state wave function and $1s$-$2s$-$2p$ close-coupling final-state continuum wave functions. Their results for the properties of the lowest ^1P helium resonances are in good agreement with the high-precision ultraviolet absorption spectra obtained by Madden and Codling.[7,8] In the present paper, the calculation of Burke and McVicar[6] is extended to the evaluation of the generalized differential oscillator strength as a function of electron energy loss and momentum transfer. This enables an investigation to be made of the effects caused by the lowest optically forbidden ^1S and ^1D helium resonances.

In 1961 Fano[9] developed a theory for the asymmetric line shapes associated with the helium resonances which have been observed in the energy-loss spectra of ionizing electrons[10,11] and in the ultraviolet absorption spectra.[7,8] The Fano line-shape formula is directly applicable to the representation of the angular dependence of the resonance features in the electron energy-loss spectra provided that the line-shape parameter q is determined as a function of momentum transfer. Resonant structure has also been observed in the angular distribution of the ejected electrons resulting from electron impact ionization of helium.[12-14] However, the interpretation of these spectra is more difficult because of the need to consider the interference between ionization amplitudes corresponding to different final-state total angular momenta and to perform the integration over the allowed range of momentum transfers.

The most stringent test of the validity of the Born approximation is provided by the spectra which are differential in all independent energy and angular variables. Such spectra have been obtained by Ehrhardt and co-workers[15,16] for the transition from the helium ground state to the ground state of the residual He^+ ion. In the present paper, the angular correlation between the scattered and the ejected electrons is expressed as an expansion in Legendre polynomial functions of the angle between

the ejected-electron momentum and the momentum-transfer vector. A comparison is made between the angular distribution predicted by the Born approximation and the coincidence measurements reported by Ehrhardt *et al.*[16] for an incident-electron energy of 256.5 eV.

II. THEORY OF DIFFERENTIAL IONIZATION CROSS SECTIONS

The calculations reported in the present paper have been restricted to the transition from the helium ground state to the $He^+(1s)$ ionization continuum below the $n=2$ threshold. In future papers this investigation will be extended to electron impact ionization from excited states of helium and to simultaneous ionization of the helium atom and excitation of the residual He^+ ion, in complete analogy with previously reported photoionization calculations.[17-22] Accordingly, it is desirable to develop a theoretical framework for the description of the more general ionization process

$$\mathrm{He}(n_0L_0S_0)+e^-(\vec{k}_0)\rightarrow \mathrm{He}^+(nl_1)+e^-(\vec{k}_n)+e^-(\vec{k}), \tag{1}$$

which involves arbitrary values of the orbital angular momenta L_0 and l_1. The incident-electron momentum is denoted by $\vec{k}_0$, whereas the faster and slower of the two outgoing electrons (which are customarily referred to as scattered and ejected) are denoted by $\vec{k}$ and $\vec{k}_n$, respectively. The subscript n on the ejected-electron momentum $\vec{k}_n$ is used to emphasize its dependence on the state of the residual He^+ ion.

In the Born approximation, only the direct scattering amplitude is considered, and the processes corresponding to exchange scattering and to capture of the incident electron are neglected. When the indistinguishability of the two outgoing electrons is taken into account, the direct, exchange, and capture amplitudes must be combined to obtain the expression for the differential cross section.[23,24]

For the collisional ionization process (1), the cross section which is differential in all independent energy and angular variables is given in the Born approximation[1,2] by the Bethe generalized oscillator strength according to the relation

$$\sigma_{nl_1}(\vec{k}_n,\vec{K})=\frac{k}{k_0}\frac{4}{EK^2}\frac{df_{nl_1,\vec{k}_n}(\vec{K})}{dE}, \tag{2}$$

where $E=k_0^2-k^2$ is the electron energy loss measured in rydbergs ($E=I+k_1^2$, where I is the ionization energy) and $\vec{K}=\vec{k}_0-\vec{k}$ is the momentum transfer. The Bethe generalized oscillator strength per unit rydberg energy interval appropriate to unpolarized atoms, ions, and electrons is given by the expression

$$\frac{df_{nl_1,\vec{k}_n}(\vec{K})}{dE}=\frac{E}{K^2}\frac{1}{2L_0+1}\sum_{M_{L_0}}\sum_{m_{l_1}}|\langle nl_1m_{l_1}\vec{k}_n|e^{i\vec{K}\cdot\vec{r}_1}+e^{i\vec{K}\cdot\vec{r}_2}|n_0L_0M_{L_0}S_0\rangle|^2, \tag{3}$$

which is to be evaluated using the spatial portions of the initial- and final-state wave functions.

After the final-continuum-state partial-wave expansion[25] satisfying the required incoming-wave boundary conditions[26] is introduced into the transition matrix elements, the generalized oscillator strength can be reduced to the Legendre polynomial expansion

$$\frac{df_{nl_1,\vec{k}_n}(\vec{K})}{dE}=\frac{1}{4\pi}\frac{df_{nl_1}(K)}{dE}\times\left(1+\sum_{L=1}^{\infty}\beta_{nl_1,L}(E,K)P_L(\cos\omega)\right), \tag{4}$$

which expresses the angular correlation between the two outgoing electrons in terms of the angle ω between the ejected-electron momentum $\vec{k}_n$ and the momentum-transfer vector $\vec{K}$. A special property of the Born approximation is that the ejected-electron angular distribution given by Eq. (4) is cylindrically symmetric about the momentum-transfer direction.

The explicit expressions which are obtained for the total generalized oscillator strength $df_{nl_1}(K)/dE$ and for the asymmetry parameters $\beta_{nl_1,L}(E,K)$ may be written in the forms

$$\frac{df_{nl_1}(K)}{dE}=\frac{E}{K^2}\frac{1}{2L_0+1}\sum_{\lambda l_2L_T}(2\lambda+1)|M(\lambda,l_2,L_T)|^2, \tag{5}$$

and

$$\frac{df_{nl_1}(K)}{dE}\beta_{nl_1,L}(E,K)=\frac{E}{K^2}\frac{(2L+1)}{(2L_0+1)}(-1)^{L_0+l_1}\sum_{\lambda l_2L_T}\sum_{\lambda' l_2'L_T'}(2\lambda+1)(2\lambda'+1)[(2l_2+1)(2l_2'+1)(2L_T+1)(2L_T'+1)]^{1/2}$$
$$\times\begin{pmatrix}l_2 & l_2' & L\\ 0 & 0 & 0\end{pmatrix}\begin{pmatrix}\lambda & \lambda' & L\\ 0 & 0 & 0\end{pmatrix}\begin{Bmatrix}l_2 & l_2' & L\\ L_T' & L_T & l_1\end{Bmatrix}\begin{Bmatrix}\lambda & \lambda' & L\\ L_T' & L_T & L_0\end{Bmatrix}M(\lambda,l_2,L_T)M(\lambda',l_2',L_T')^*, \tag{6}$$

where

$$M(\lambda, l_2, L_T) = i^{\lambda} e^{i(\sigma_{l_2} - l_2\pi/2)} (n l_1 l_2, L_T S_0 || j_\lambda(Kr_1) C^{(\lambda)}(\hat{r}_1) + j_\lambda(Kr_2) C^{(\lambda)}(\hat{r}_2) || n_0 L_0 S_0) . \quad (7)$$

σ_{l_2} denotes the Coulomb phase shift for the He^+ ion, $j_\lambda(Kr)$ is the spherical Bessel function, and $C^{(\lambda)}(\hat{r})$ is the Racah tensor operator. In the above reduced matrix elements, the final-continuum states are characterized by the channel quantum numbers $n l_1 l_2, L_T S_0$, where l_2 is the ejected-electron relative orbital angular momentum and L_T is the total orbital angular momentum. Moreover, the continuum wave functions are normalized per unit energy in rydbergs. It is important to note that in the Born approximation only those final states with the same total spin S_0 as the initial helium state are excited in the ionizing collision. The summations in Eqs. (5) and (6) are to be taken over all values of the angular momenta which are consistent with the selection rules associated with the 3-j and 6-j symbols. For the transition

$$He(1\,^1S) \rightarrow He^+(1s) + e^-(l_2), \quad \lambda = l_2 = L_T .$$

In the limit $\vec{K} \rightarrow 0$, $\lambda = 1$ and only the $L = 2$ term occurs in the Legendre polynomial expansion. The oscillator strength obtained from Eq. (4) in the limit of zero momentum transfer describes photoionization by linearly polarized electric-dipole photons, a result which is in complete agreement with the work of Kim.[27] The resulting expression for the asymmetry parameter is in agreement with the relation obtained previously for photoionization.[20]

III. CALCULATIONS

The first six partial-wave contributions ($0 \leq L_T \leq 5$) to the generalized oscillator strength $df_{1s,\vec{k}_1}(\vec{K})/dE$ were evaluated for ejected-electron energies in the range $0.2 \leq k_1^2 \leq 2.8$ Ry using a 56-term Hylleraas expansion[17] for the helium ground-state wave function and $1s$-$2s$-$2p$ close-coupling final-state continuum wave functions.[6] The procedure originally developed for photoionization calculations[6,17] has been extended to express the reduced electron impact ionization amplitudes $M(\lambda, l_2, L_T)$ as a sum (over all final-state channels included in the close-coupling expansion) of integrals involving the ejected-electron radial wave functions and the associated (momentum-transfer dependent) ground-state weight functions.

In the usual definition of the generalized oscillator strength given by Eq. (3), it is customary to omit the contribution arising from the Coulomb interaction between the incident electron and the nuclear charge. This contribution vanishes because of the assumption that the initial- and final-state wave functions are exactly orthogonal. In the present calculation, it was found necessary to include this interaction in the evaluation of the S partial-wave amplitude in order to eliminate the small but nonzero overlap term which would lead to incorrect results for small momentum transfers. The alternative procedure of orthogonalizing the initial- and final-state wave functions may lead to different results.

IV. RESULTS AND DISCUSSION

A. Nonresonant energy-loss spectra

The differential ionization cross section appropriate to the detection of the scattered electron in a given direction, without regard for the ejected-electron direction, is proportional to the total generalized oscillator strength $df_{1s}(K)/dE$. The results obtained for $df_{1s}(K)/dE$ (per unit rydberg energy interval) are presented in Table I as a function of the ejected-electron energy k_1^2 and of the magnitude of the momentum transfer K. In the nonresonant region the present results for $df_{1s}(K)/dE$ do not differ by more than 5% from the values calculated by Oldham[28] and by Bell and Kingston,[29] who employed less sophisticated initial- and final-state wave functions in their evaluations of the Born ionization amplitude. In addition, these two previous calculations[28,29] are in good agreement with the nonresonant energy-loss spectra obtained experimentally by Silverman and Lassettre[10] at an incident-electron energy of 500 eV.

The most important qualitative features of the nonresonant energy-loss spectra are illustrated in Fig. 1, where the total generalized oscillator strength for representative momentum transfers is plotted as a function of the ejected-electron energy and of the corresponding energy loss. The $K = 0$ curve is the differential oscillator strength for photoionization of helium previously calculated.[6,17]

For small K, the generalized oscillator strength decreases rapidly with increasing energy loss, and the value at the ionization threshold also decreases rapidly with increasing momentum transfer. As K increases beyond 1.0 a.u., a second peak may be seen to develop at approximately $k_1^2 = K^2$. The occurrence of this peak can be explained in terms of energy and momentum conservation in the free-electron limit.

TABLE I. Total generalized oscillator strength $df_{1s}(K)/dE$ for ionization of helium (per unit rydberg energy interval).

k_1^2 (Ry)	K (a.u.) 0.2	0.4	0.6	0.8	1.0	1.2	1.4
0.2	0.7707	0.7383	0.6707	0.5669	0.4421	0.3197	0.2173
0.4	0.6661	0.6597	0.6304	0.5659	0.4692	0.3583	0.2543
0.6	0.5767	0.5849	0.5813	0.5489	0.4811	0.3874	0.2877
0.8	0.5016	0.5174	0.5298	0.5218	0.4805	0.4070	0.3163
1.0	0.4390	0.4581	0.4798	0.4891	0.4703	0.4175	0.3393
1.2	0.3866	0.4066	0.4331	0.4537	0.4528	0.4195	0.3561
1.4	0.3421	0.3618	0.3901	0.4177	0.4303	0.4145	0.3665
1.6	0.3048	0.3236	0.3520	0.3833	0.4055	0.4043	0.3716
1.8	0.2728	0.2904	0.3179	0.3503	0.3794	0.3900	0.3716
2.0	0.2457	0.2620	0.2881	0.3212	0.3537	0.3734	0.3677
2.2	0.2234	0.2383	0.2628	0.2951	0.3297	0.3560	0.3612
2.4	0.2064	0.2206	0.2441	0.2759	0.3120	0.3437	0.3587
2.45	0.2032	0.2157	0.2357	0.2617	0.2901	0.3134	0.3209
2.5	0.2024	0.2146	0.2352	0.2636	0.2969	0.3274	0.3434
2.55	0.2066	0.2186	0.2389	0.2671	0.3004	0.3318	0.3498
2.6	0.2498	0.2593	0.2754	0.2983	0.3267	0.3556	0.3752
2.65	0.1301	0.1427	0.1641	0.1940	0.2300	0.2657	0.2903
2.7	0.1577	0.1697	0.1900	0.2186	0.2533	0.2881	0.3125
2.75	0.1621	0.1737	0.1935	0.2214	0.2556	0.2905	0.3160
2.8	0.1645	0.1760	0.1953	0.2227	0.2565	0.2914	0.3179

B. Resonant energy-loss spectra

The spectral features associated with the $(2s^2)\,^1S$, $(2s2p)\,^1P$, and $(2p^2)\,^1D$ helium autoionizing states are illustrated for three different momentum transfers in Fig. 2. The most prominent peak corresponds to the optically allowed excitation of the $(2s2p)\,^1P$ state. The optically forbidden transitions to the $(2s^2)\,^1S$ and $(2p^2)\,^1D$ states become increasingly visible for larger momentum transfers. The $(2s2p)\,^1P$ feature shows the asymmetry observed by Silverman and Lassettre,[10] while the $(2s^2)\,^1S$ and $(2p^2)\,^1D$ features are qualitatively similar to those detected by Simpson *et al.*[11] The ob-

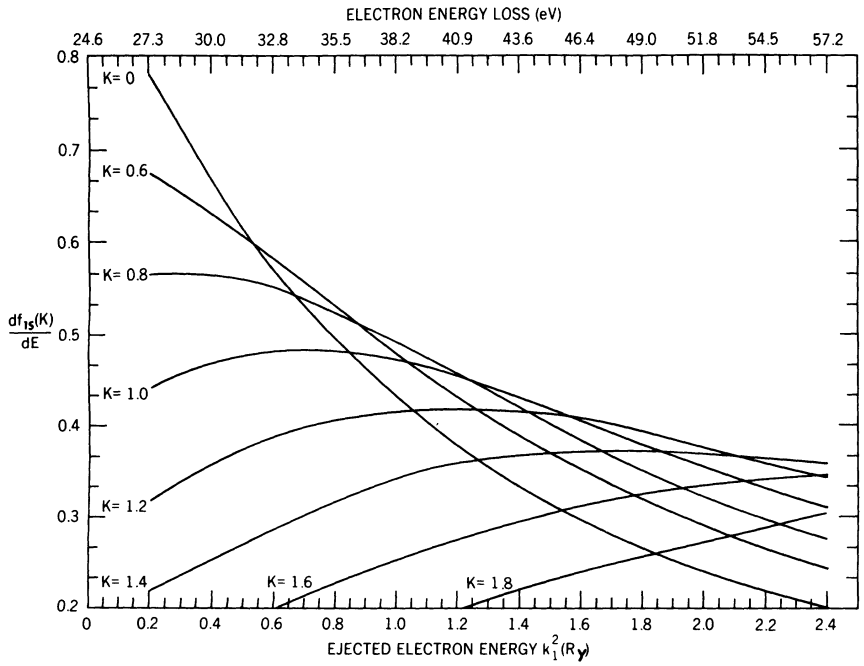

FIG. 1. Total generalized oscillator strength (per unit rydberg energy interval) for nonresonant electron impact ionization of helium.

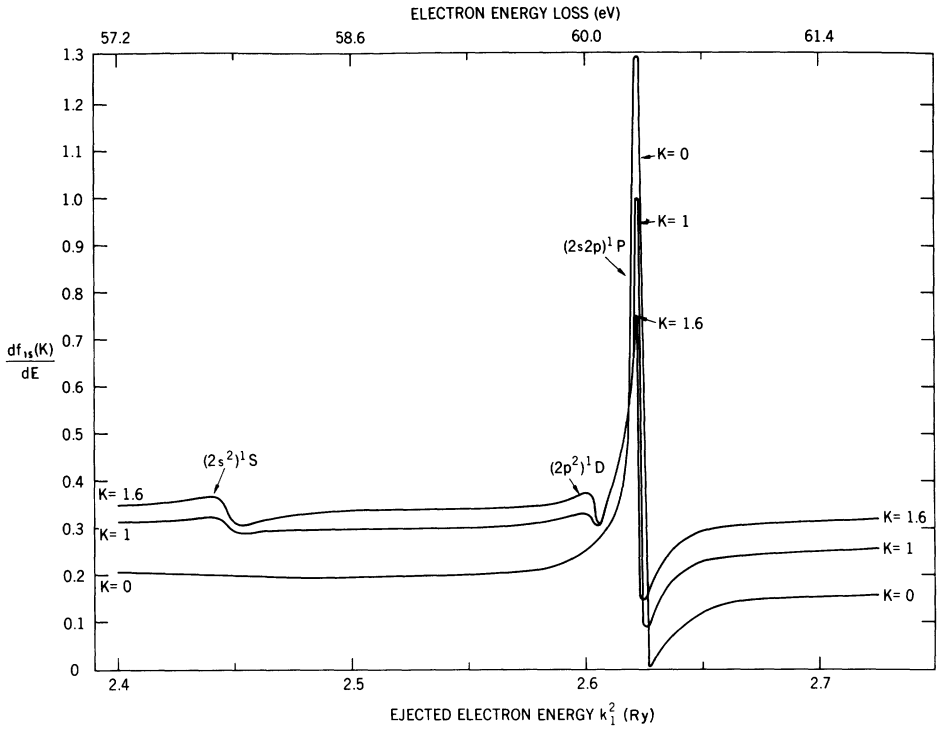

FIG. 2. Total generalized oscillator strength (per unit rydberg energy interval) for resonant electron impact ionization of helium.

served energy-loss spectra[10,11] refer to a zero scattering angle, but the corresponding momentum transfers are not sufficiently close to the zero limit to justify the neglect of the optically forbidden transitions in the interpretation of the experimental data.

Fano[9] has shown that the asymmetric line shape observed by Silverman and Lassettre[10] is caused by the interference between the resonant and the nonresonant contributions to the ionization amplitude associated with a given angular momentum. In the vicinity of an isolated resonance in the L_T partial-wave continuum channel, the total generalized oscillator strength may be represented by the form

$$\frac{df_{1s}(K)}{dE} = \left(\frac{df_{1s,L_T}(K)}{dE}\right)_0 \frac{[\epsilon + q_{L_T}(K)]^2}{1+\epsilon^2} + \sum_{L_T' \neq L_T} \frac{df_{1s,L_T'}(K)}{dE}, \tag{8}$$

where ϵ is defined in terms of the resonance position E_r and the width Γ_r according to the relation

$$\epsilon = 2(E - E_r)/\Gamma_r . \tag{9}$$

The rapid variation through the resonance is determined by the line-profile parameter $q_{L_T}(K)$, while the nonresonant background oscillator strength $(df_{1s,L_T}(K)/dE)_0$ and the contributions from the other angular momenta $L_T' \neq L_T$ are assumed to vary slowly with ϵ. The variation of the generalized oscillator strength in the neighborhood of the $(2s^2)^1S$ resonance is accurately described by Eq. (8). To provide a realistic interpretation of the energy-loss spectra near 60 eV, the effects of the $(2p^2)^1D$ and $(2s2p)^1P$ resonances (which are separated by only 0.24 eV) must be superimposed according to the relation

$$\frac{df_{1s}(K)}{dE} = \sum_{L_T=1,2} \left(\frac{df_{1s,L_T}(K)}{dE}\right)_0 \frac{[\epsilon + q_{L_T}(K)]^2}{1+\epsilon^2} + \sum_{L_T' \neq 1,2} \frac{df_{1s,L_T'}(K)}{dE} \tag{10}$$

The $(2s^2)^1S$, $(2s2p)^1P$, and $(2p^2)^1D$ resonance parameters were determined by fitting the respective generalized partial-wave oscillator strengths to the Fano line-shape formula [the first term in Eq. (8)]. The positions and widths obtained in the $1s$-$2s$-$2p$ close-coupling approximation by Burke[30] were used in the analysis. The nonresonant background oscillator strength $(df_{1s,L_T}(K)/dE)_0$ was allowed to vary linearly with ϵ, but the linear coefficient was found to be at least two orders of magnitude smaller than the ϵ-independent term in all cases considered. The line-profile parameter

$q_{L_T}(K)$, the nonresonant background oscillator strength (evaluated at $\epsilon = 0$), and the slowly varying sum of the other angular-momentum contributions [defined either by Eq. (8) or by Eq. (10)] which were obtained for the lowest three resonances are presented as functions of K in Table II. For $K = 0$, the $(2s2p)\,^1P$ resonance parameters obtained by Burke and McVicar[6] are quoted.

The most surprising result of the resonance analysis is the prediction, in all three cases considered, of a minimum value of $|q_{L_T}(K)|$ within the range $0 < K < 2$. Using less sophisticated helium wave functions, Balashov *et al.*[31] have obtained results for the $(2s2p)\,^1P$ line-profile parameter which are in qualitative agreement with the present calculation.

TABLE II. Parameters for the lowest three resonances in the total generalized oscillator strength for ionization of helium. The numbers in parentheses are the powers of 10 by which the entries are to be multiplied.

K (a.u.)	$q_{L_T}(K)$	$\left(\frac{df_{1s,L_T}(K)}{dE}\right)_0$	$\sum_{L_T'} \frac{df_{1s,L_T'}(K)}{dE}$
	$(2s^2)\,^1S$		$L_T' \neq 0$
0.4	−2.10	0.371(−3)	0.214
0.6	−1.89	0.293(−2)	0.233
0.8	−1.50	0.764(−2)	0.259
1.0	−1.29	0.136(−1)	0.287
1.2	−1.14	0.209(−1)	0.311
1.4	−1.05	0.285(−1)	0.319
1.6	−1.00	0.349(−1)	0.302
1.8	−1.01	0.384(−1)	0.259
2.0	−1.05	0.381(−1)	0.203
	$(2s2p)\,^1P$		$L_T' \neq 1, 2$
0	−2.59[a]	0.175[a]	0
0.2	−2.46	0.183	0.456(−3)
0.4	−2.37	0.186	0.215(−2)
0.6	−2.23	0.191	0.598(−2)
0.8	−2.06	0.196	0.132(−1)
1.0	−1.90	0.201	0.250(−1)
1.2	−1.75	0.202	0.409(−1)
1.4	−1.65	0.195	0.576(−1)
1.6	−1.61	0.179	0.697(−1)
1.8	−1.62	0.153	0.729(−1)
2.0	−1.68	0.121	0.670(−1)
	$(2p^2)\,^1D$		$L_T' \neq 1, 2$
0.4	−0.149	0.119(−1)	0.215(−2)
0.6	−0.083	0.207(−1)	0.600(−2)
0.8	−0.073	0.345(−1)	0.133(−1)
1.0	−0.107	0.542(−1)	0.251(−1)
1.2	−0.138	0.673(−1)	0.410(−1)
1.4	−0.214	0.812(−1)	0.576(−1)
1.6	−0.297	0.803(−1)	0.695(−1)
1.8	−0.408	0.751(−1)	0.725(−1)
2.0	−0.529	0.588(−1)	0.666(−1)

[a] Reference 6.

C. Angular correlation between the two outgoing electrons

The angular correlation between the scattered and the ejected electrons, which is given by

$$W(\omega) = 1 + \sum_{L=1}^{\infty} \beta_{1s,L}(k_1^2, K) P_L(\cos\omega), \tag{11}$$

may be evaluated for a wide range of the independent dynamical variables using the asymmetry parameters $\beta_{1s,L}(k_1^2, K)$ presented (for $L = 1, 5$) in Table III. The angle ω between the ejected-electron direction and the momentum-transfer vector may be expressed in terms of the respective polar angles as follows:

$$\cos\omega = \cos\theta_{k_1}\cos\theta_K + \sin\theta_{k_1}\sin\theta_K\cos(\phi_{k_1} - \phi_K), \tag{12}$$

where

$$\cos\theta_K = \frac{K^2 + E}{2Kk_0} = \frac{K^2 + k_1^2 + I}{2Kk_0}. \tag{13}$$

The angular distributions obtained experimentally by Ehrhardt *et al.*[15,16] have been presented in the form of polar plots as functions of θ_{k_1}. A comparison of the angular distribution predicted by the present calculation with the coincidence mea-

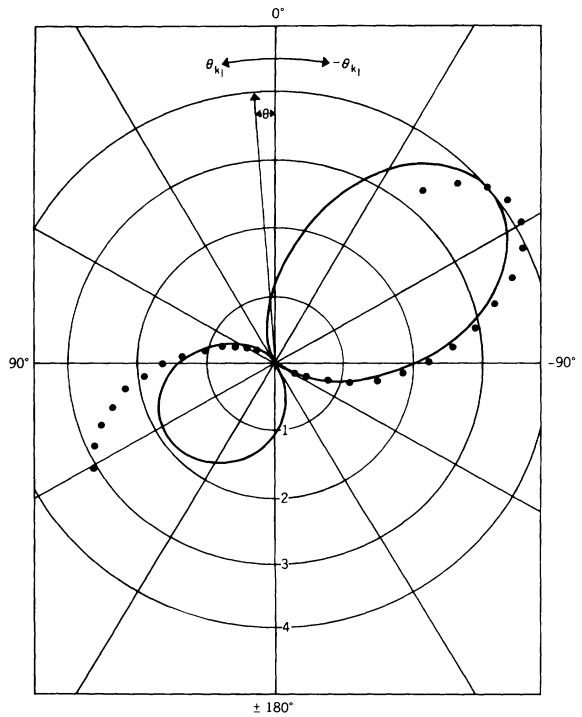

FIG. 3. Angular distribution of the ejected electrons resulting from ionization of helium by 256.5-eV incident electrons. The ejected-electron energy k_1^2 is 3.0 eV and the scattering angle θ is 4°. Solid curve, present calculation; closed circles, Ehrhardt *et al.* (Ref. 16).

TABLE III. Angular distribution expansion coefficients $\beta_{1s,L}(k_1^2,K)$ for ionization of helium. The numbers in parentheses are the powers of ten by which the entries are to be multiplied.

k_1^2(Ry)	$L=1$	$L=2$	$L=3$	$L=4$	$L=5$
			$K=0.2$ a.u.		
0.2	2.270(−1)	1.958	3.472(−1)	3.458(−2)	2.737(−3)
0.4	3.283(−1)	1.981	4.396(−1)	5.760(−2)	5.963(−3)
0.6	3.812(−1)	1.999	4.885(−1)	7.260(−2)	8.604(−3)
0.8	4.142(−1)	2.010	5.149(−1)	8.187(−2)	1.047(−2)
1.0	4.362(−1)	2.018	5.289(−1)	8.727(−2)	1.166(−2)
1.2	4.474(−1)	2.024	5.355(−1)	9.009(−2)	1.234(−2)
1.4	4.499(−1)	2.029	5.378(−1)	9.130(−2)	1.266(−2)
1.6	4.494(−1)	2.032	5.367(−1)	9.131(−2)	1.272(−2)
1.8	4.524(−1)	2.033	5.337(−1)	9.061(−2)	1.261(−2)
2.0	4.580(−1)	2.034	5.291(−1)	8.935(−2)	1.238(−2)
2.2	4.602(−1)	2.034	5.224(−1)	8.747(−2)	1.204(−2)
2.4	4.528(−1)	2.031	5.119(−1)	8.458(−2)	1.152(−2)
2.45	1.843(−1)	2.005	5.069(−1)	8.354(−2)	1.135(−2)
2.5	4.352(−1)	2.037	5.043(−1)	8.217(−2)	1.109(−2)
2.6	3.674(−1)	2.037	4.076(−1)	6.296(−2)	7.253(−3)
2.625	−5.625(−1)	1.916	−8.257(−1)	−3.844(−3)	1.035(−2)
			$K=0.4$ a.u.		
0.2	4.169(−1)	1.847	6.156(−1)	1.168(−1)	1.760(−2)
0.4	6.110(−1)	1.929	7.951(−1)	1.980(−1)	3.926(−2)
0.6	7.182(−1)	1.992	9.000(−1)	2.544(−1)	5.779(−2)
0.8	7.843(−1)	2.036	9.639(−1)	2.922(−1)	7.170(−2)
1.0	8.261(−1)	2.067	1.003	3.164(−1)	8.129(−2)
1.2	8.513(−1)	2.089	1.026	3.311(−1)	8.737(−2)
1.4	8.649(−1)	2.106	1.038	3.393(−1)	9.085(−2)
1.6	8.714(−1)	2.118	1.043	3.424(−1)	9.230(−2)
1.8	8.764(−1)	2.125	1.042	3.423(−1)	9.238(−2)
2.0	8.798(−1)	2.130	1.037	3.395(−1)	9.140(−2)
2.2	8.785(−1)	2.132	1.027	3.340(−1)	8.943(−2)
2.4	8.650(−1)	2.121	1.006	3.234(−1)	8.584(−2)
2.45	3.872(−1)	2.030	9.915(−1)	3.204(−1)	8.509(−2)
2.5	8.438(−1)	2.143	1.001	3.178(−1)	8.360(−2)
2.6	7.203(−1)	2.144	8.136(−1)	2.464(−1)	5.562(−2)
2.625	−9.859(−1)	1.694	−1.504	3.481(−2)	9.568(−2)
			$K=0.6$ a.u.		
0.2	5.488(−1)	1.693	7.712(−1)	2.030(−1)	4.255(−2)
0.4	8.221(−1)	1.851	1.025	3.536(−1)	9.821(−2)
0.6	9.791(−1)	1.972	1.191	4.667(−1)	1.486(−1)
0.8	1.079	2.061	1.304	5.494(−1)	1.893(−1)
1.0	1.145	2.126	1.381	6.084(−1)	2.201(−1)
1.2	1.187	2.175	1.434	6.491(−1)	2.419(−1)
1.4	1.214	2.211	1.469	6.762(−1)	2.566(−1)
1.6	1.230	2.237	1.490	6.920(−1)	2.652(−1)
1.8	1.241	2.256	1.501	6.997(−1)	2.693(−1)
2.0	1.247	2.267	1.504	7.007(−1)	2.698(−1)
2.2	1.246	2.274	1.497	6.950(−1)	2.668(−1)
2.4	1.225	2.252	1.466	6.752(−1)	2.576(−1)
2.45	6.310(−1)	2.100	1.446	6.755(−1)	2.590(−1)
2.5	1.217	2.300	1.481	6.742(−1)	2.552(−1)
2.6	1.048	2.305	1.217	5.339(−1)	1.745(−1)
2.625	−1.051	1.463	−1.726	2.516(−1)	3.657(−1)
			$K=0.8$ a.u.		
0.2	6.204(−1)	1.521	8.244(−1)	2.167(−1)	6.630(−2)
0.4	9.570(−1)	1.751	1.134	4.709(−1)	1.594(−1)
0.6	1.157	1.932	1.356	6.407(−1)	2.490(−1)

TABLE III *(continued)*

k_1^2(Ry)	$L=1$	$L=2$	$L=3$	$L=4$	$L=5$
			$K=0.8$ a.u.		
0.8	1.289	2.069	1.521	7.753(−1)	3.267(−1)
1.0	1.379	2.174	1.645	8.798(−1)	3.902(−1)
1.2	1.441	2.254	1.737	9.593(−1)	4.400(−1)
1.4	1.484	2.316	1.806	1.019	4.776(−1)
1.6	1.512	2.362	1.855	1.060	5.041(−1)
1.8	1.532	2.396	1.887	1.088	5.214(−1)
2.0	1.544	2.420	1.906	1.103	5.308(−1)
2.2	1.547	2.434	1.912	1.106	5.325(−1)
2.4	1.519	2.404	1.875	1.081	5.190(−1)
2.45	9.033(−1)	2.225	1.870	1.102	5.336(−1)
2.5	1.537	2.486	1.924	1.099	5.241(−1)
2.6	1.344	2.498	1.610	8.949(−1)	3.709(−1)
2.625	−6.307(−1)	1.419	−1.230	7.329(−1)	8.683(−1)

surements of Ehrhardt *et al.*[16] is shown in Fig. 3, where the experimental results have been normalized to the theoretical values near the forward maximum. The incident- and ejected-electron energies are $k_0^2=256.5$ eV and $k_1^2=3.0$ eV, and the scattering angle (which is indicated by the arrow in Fig. 3) is $\theta=4°$. In the experiment, the ejected electrons were detected only in the scattering plane defined by $\vec{k}_0$ and $\vec{k}$, and θ_{k_1} is taken to be negative when the two outgoing electrons are detected on opposite sides of the incident-electron direction.

The forward ($\theta_{k_1}\sim -60°$) and backward ($\theta_{k_1}\sim +140°$) maxima have been called the binary encounter and the recoil peaks, respectively. The agreement between the experimentally determined angular distribution and the theoretical results is satisfactory except in the backward direction, where the theoretical value at the recoil peak is about 30% less than the relative experimental intensity. In addition, the symmetry axis that is common to the observed maxima is shifted away from the momentum-transfer direction by 4.6°, indicating a further inadequacy of the Born approximation. Schulz[32] has found that the inclusion of the exchange and capture amplitudes improves the theoretical predictions at high incident-electron energies by increasing the angle of the forward maximum and lowering the intensity at the binary peak.

ACKNOWLEDGMENTS

The author is indebted to Professor P. G. Burke for his numerous suggestions and for the use of his close-coupling program. Many helpful discussions with Dr. M. Inokuti, Dr. Y.-K. Kim, Dr. K. Omidvar, and Dr. A. Temkin are gratefully acknowledged. Finally, the author expresses his gratitude to Dr. M. Schulz for communicating the experimental data.

*National Academy of Sciences, National Research Council, Resident Research Associate.

[1]H. Bethe, Ann. Phys. (Leipz.) 5, 325 (1930).
[2]M. Inokuti, Rev. Mod. Phys. 43, 297 (1971).
[3]Y.-K. Kim and M. Inokuti, Phys. Rev. 175, 176 (1968).
[4]Y.-K. Kim and M. Inokuti, Phys. Rev. 181, 205 (1969).
[5]Y.-K. Kim and M. Inokuti, Phys. Rev. 184, 38 (1969).
[6]P. G. Burke and D. D. McVicar, Proc. Phys. Soc. Lond. 80, 616 (1962).
[7]R. P. Madden and K. Codling, Phys. Rev. Lett. 10, 516 (1963).
[8]R. P. Madden and K. Codling, Astrophys. J. 141, 364 (1965).
[9]U. Fano, Phys. Rev. 124, 1866 (1961).
[10]S. M. Silverman and E. N. Lassettre, J. Chem. Phys. 40, 1265 (1964).
[11]J. A. Simpson, G. E. Chamberlain, and S. R. Mielczarek, Phys. Rev. A 139, 1039 (1965).
[12]W. Mehlhorn, Phys. Rev. Lett. 21, 155 (1966).
[13]N. Oda, F. Nishimura, and S. Tahira, Phys. Rev. Lett. 24, 42 (1970).
[14]G. B. Crooks and M. E. Rudd, in *Proceedings of the Seventh International Conference on the Physics of Electronic and Atomic Collisions, 1971*, edited by L. M. Branscomb *et al.* (North-Holland, Amsterdam, 1972), p. 1035.
[15]H. Ehrhardt, K. H. Hesselbacher, K. Jung, and K. Willmann, *Case Studies in Atomic Collision Physics II* (North-Holland, Amsterdam, 1972).
[16]H. Ehrhardt, K. H. Hesselbacher, K. Jung, M. Schulz, and K. Willmann, J. Phys. B 5, 2107 (1972).
[17]V. L. Jacobs, Phys. Rev. A 3, 289 (1971).
[18]V. L. Jacobs, Phys. Rev. A 4, 939 (1972).
[19]V. L. Jacobs, Phys. Rev. A 9, 1938 (1974).

[20]V. L. Jacobs and P. G. Burke, J. Phys. B 5, L67 (1972).
[21]V. L. Jacobs and P. G. Burke, J. Phys. B 5, 2272 (1972).
[22]H. A. Hyman, V. L. Jacobs, and P. G. Burke, J. Phys. B 5, 2282 (1972).
[23]M. R. H. Rudge, Rev. Mod. Phys. 40, 564 (1968).
[24]D. H. Phillips and M. R. C. McDowell, J. Phys. B 6, L165 (1973).
[25]V. L. Jacobs, J. Phys. B 6, 1461 (1973).
[26]G. Breit and H. Bethe, Phys. Rev. 93, 888 (1954).
[27]Y.-K. Kim, Phys. Rev. A 6, 666 (1972).
[28]W. J. B. Oldham, Phys. Rev. 186, 52 (1969).
[29]K. L. Bell and A. E. Kingston, J. Phys. B 3, 1300 (1970).
[30]P. G. Burke, *Advances in Atomic and Molecular Physics* (Academic, New York, 1968), Vol. 4.
[31]V. V. Balashov, S. S. Lipovetsky, A. V. Pavlitchenkov, A. N. Polyudov, and V. S. Sena Shenko, in Ref. 14, p. 1028.
[32]M. Schulz, J. Phys. B 6, 2580 (1973).